Chinese Chemical Letters 33 (2022) 3581–3584

Contents lists available at ScienceDirect

Chinese Chemical Letters

journal homepage: www.elsevier.com/locate/cclet

Efficient photoreduction strategy for uranium immobilization based on graphite carbon nitride/activated carbon nanocomposites

Shuyang Li[b], Zhiwei Niu[b,c], Duoqiang Pan[a,b,*], Zhenpeng Cui[b], Hewen Shang[b], Jie Lian[b], Wangsuo Wu[a,c,*]

[a] Frontiers Science Center for Rare Isotopes, Lanzhou University, Lanzhou 730000, China
[b] School of Nuclear Science and Technology, Lanzhou University, Lanzhou 730000, China
[c] Key Laboratory of Special Function Materials and Structure Design, Ministry of Education, Lanzhou 730000, China

ARTICLE INFO

Article history:
Received 24 December 2021
Revised 7 March 2022
Accepted 10 March 2022
Available online 13 March 2022

Keywords:
Uranium removal
Photoreduction
Graphitic carbon nitride
Activated carbon
Composite material

ABSTRACT

Uranium removal from aqueous solutions using environmentally friendly photocatalytic technology is a novel approach for resource recovery. Herein, carbon nitride/activated carbon composite materials (CN/AC) were investigated for U(VI) reduction under visible light. An exceptional boost in photocatalytic activity was observed for CN/AC composites (up to 70 times over the conventional bulk g-C_3N_4). The strong interactive conjugated π-bond structure between g-C_3N_4 and AC accelerated the migration of carriers and then prolonged the electron lifetime. CN/AC composites exhibited excellent compatibility with different water substrates and were resilience to a wide range of pH changes and abundant competitive anions/cations. Quenching experiments and electron microscopy characterization indicated that U(VI) was reduced by photogenerated electrons and deposited on the edge of CN/AC composites. The low-cost, high-performance carbon-based composite material proposed in this work is a potential candidate for the efficient treatment of radioactive wastewater.

Uranium is the main fuel used to produce nuclear power and its production is necessary to guarantee the sustainable development of the nuclear industry [1,2]. However, the radioactive and chemical toxicity of uranium presents a potential hazard to the environment [3,4]. Therefore, the enrichment and removal of uranium are critical to resource recovery and environmental purification. Adsorption is an important means of uranium removal [5,6]. However, the adsorption capacity of a material depends largely on the specific surface area and adsorption sites of the material. The inherent limitations of the adsorption method limit its wide application [7–10]. Therefore, the development of novel technologies and strategies for uranium immobilization remains a central challenge.

Photocatalytic technology driven by economical and environmentally friendly solar energy can reduce easily soluble hexavalent uranium (U(VI)) to insoluble tetravalent uranium (U(IV)) precipitates to achieve purification and recovery [11–14]. The key factor determining reduction performance is well-known to be the reasonable design of a photocatalyst. Graphitic carbon nitride (g-C_3N_4) has been widely used in the study of U(VI) reduction but has some inherent defects: i) weak photocatalytic activity under visible light, ii) a high recombination rate of photogenerated electron-hole pairs, and iii) a low specific surface area [15,16]. Consequently, extensive effort has been expended to develop methods to modify photocatalysts that improve U(VI) reduction performance, such as structural modification, elemental doping, and composite construction [17–19]. Among these methods, the construction of composite materials can effectively inhibit the rapid recombination of photogenerated carriers in a system, accelerate electron transfer, and improve photocatalytic activity.

Carbon materials, such as graphene, porous carbon, activated carbon, and carbon nanotubes, have been widely investigated and applied [20–22]. For instance, carbon nitride/graphene oxide (g-C_3N_4/GO) composites synthesized by ultrasonic treatment exhibited enhanced U(VI) extraction ability under simulated sunlight compared to that of pristine g-C_3N_4 and GO. However, the GO manufacturing process is complex and not economically competitive. Furthermore, toxic substances may be used in the synthesis process that can cause secondary pollution in the environment. By sharp contrast, activated carbon (AC) has abundant pores and surface functional groups, while being easier to prepare and cost-effective [23]. However, AC is rarely regarded as a candidate

* Corresponding authors.
E-mail addresses: panduoqiang@lzu.edu.cn (D. Pan), wuws@lzu.edu.cn (W. Wu).

https://doi.org/10.1016/j.cclet.2022.03.043
1001-8417/

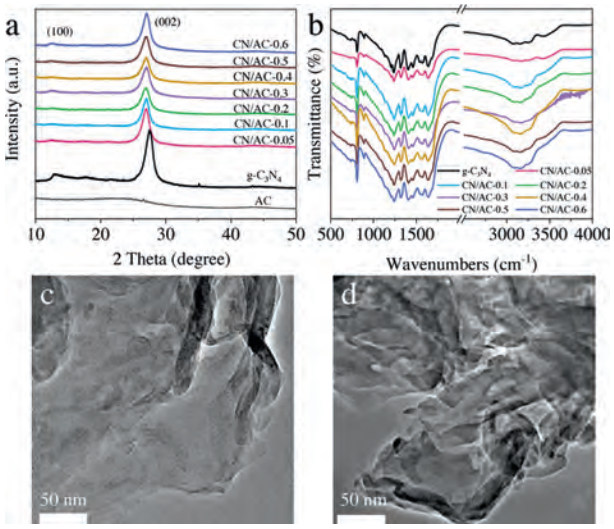

Fig. 1. Characterization of catalysts. (a) XRD patterns and (b) FT-IR spectra of the CN/AC composites; TEM images of (c) g-C_3N_4 and (d) CN/AC-0.3.

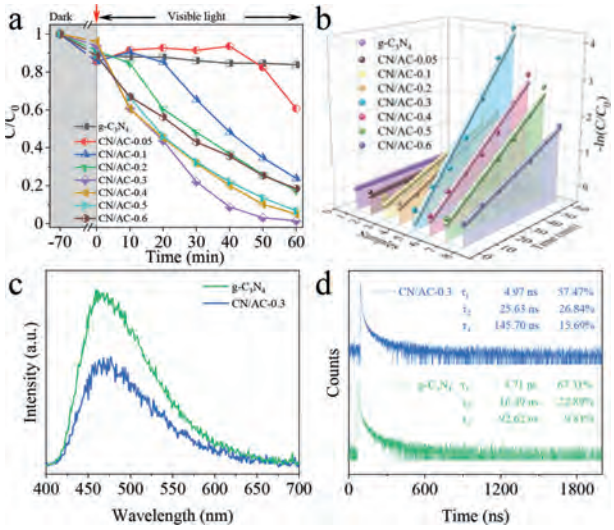

Fig. 2. The photocatalytic performance of the as-synthesized catalysts. (a) Comparison of photoreduction performance of CN/AC catalysts for U(VI). (b) The *pseudo*-first-order rate constant of U(VI) reduction by CN/AC catalysts. (c) PL spectra and (d) time-resolved PL spectra of g-C_3N_4 and CN/AC-0.3.

for constructing photocatalytic composites. Coincidentally, AC and g-C_3N_4 are carbon-based materials with the same π-conjugated structure and can therefore form a strong interactive structure of conjugated π-bonds. Studies have shown that the strong interaction between carbon-based materials and g-C_3N_4 caused by conjugative π-bonds can improve photocatalytic activity [24,25]. This strong interaction can be exploited to accelerate the separation and transfer of photogenerated carriers to achieve efficient U(VI) reduction under visible light.

Herein, we successfully constructed graphitic carbon nitride/activated carbon (CN/AC) composite materials for U(VI) reduction under visible light. The photoreduction ability of the CN/AC composites for U(VI) was systematically investigated under different water chemistry conditions. The strongly interacting conjugated π-bond structure formed between g-C_3N_4 and AC enabled enhanced U(VI) removal capability for the CN/AC composites (70 times that of pristine g-C_3N_4). The excellent reduction performance of CN/AC composites under visible light indicated a high application potential for uranium enrichment/removal, making these composites novel potential radioactive wastewater treatment materials.

The crystal phase structure, as identified by XRD, was shown in Fig. 1a. The in-plane structure packing motif and interlayer stacking reaction of the aromatic system produced two distinct characteristic peaks at 13.1° and 27.4°, corresponding to the (100) and (002) crystal planes of g-C_3N_4, respectively. Note that with increasing AC content, the peak intensity in spectra of the CN/AC catalysts gradually decreased, and the characteristic peaks gradually shifted to a low angle. This result was attributed to the introduction of amorphous AC, which reduced the crystallinity of the CN/AC composites but did not change the C–N framework of g-C_3N_4. The result also indicated that the introduction of AC increases the g-C_3N_4 layer spacing, inhibited stacking of the g-C_3N_4 layer to expand the contact area between CN/AC composites and the target, and increased the number of reaction sites. A detailed analysis of the functional groups of the catalyst was performed using Fourier transform infrared spectroscopy (FT-IR). Fig. 1b showed characteristic peaks of g-C_3N_4 in the spectra of all the samples, indicating that the chemical structure was not significantly changed. The typical absorption peak at 808 cm^{-1} represented the breathing mode of the triazine unit, whereas the characteristic peak in the range of 1200∼1800 cm^{-1} corresponded to the stretching modes of the aromatic g-C_3N_4 heterocycles. The broad absorption band at ∼3000∼3500 cm^{-1} may reflect the stretching vibration modes of N–H and hydroxyl groups of adsorbed water. The band intensity increased with the AC content, which indicated that CN/AC composites had a larger specific surface area and can absorb more H_2O than g-C_3N_4.

The chemical states of the catalyst surface were further observed by XPS (Fig. S1 in Supporting information). The C 1s peaks located at 284.6 and 288 eV correspond to sp^2 C–C and N–C=N, respectively. The N 1s peaks of g-C_3N_4 are attributed to N=C–N (sp^2-hybridized nitrogen), N-$(C)_3$ (tertiary nitrogen bonded to carbon), C–N–H (an amino-functional group), and charge effects in heterocycles. Note that the CN/AC-0.3 spectrum was shifted toward higher binding energy than that of g-C_3N_4. This phenomenon implied a strong interaction between g-C_3N_4 and AC.

Figs. 1c and d showed the morphological structures of g-C_3N_4 and CN/AC-0.3, respectively. The g-C_3N_4 had a thick and compact flake structure, whereas CN/AC-0.3 had a thinner and lighter two-dimensional layered nanosheet structure. This result could indicate that the introduction of AC during the thermal etching of melamine contributes to the formation of ultrathin nanosheet structures. The morphology of CN/AC-0.3 was consistent with the XRD analysis results. The increase in the g-C_3N_4 layer spacing resulted in the formation of thinner and lighter nanosheets.

The photocatalytic performance enhanced by CN/AC composites was confirmed by performing uranium removal experiments under visible light. Fig. 2a showed that in an aqueous solution of pH 5, g-C_3N_4 had almost no reducing ability toward U(VI). This result was attributed to the rapid recombination of photogenerated electron-hole pairs in bulk g-C_3N_4, such that there were insufficient electrons to participate in the uranium reduction reaction. The photoreduction ability of the CN/AC composites improved as the quantity of AC introduced increased. CN/AC-0.3 (corresponding to 0.3 g of added AC) exhibited an optimal removal effect as high as 98.5%. The uranium removal capability of CN/AC-0.3 was competitive with those of reported materials (Table S1 in Supporting information). However, adding more than 0.3 g of AC to the CN/AC composites weakened the photoreduction ability. This result may have been obtained because excessive AC can cover g-C_3N_4 and affect visible light absorption. The corresponding reaction rate was calculated using a *pseudo*-first-order kinetic model ($-\ln(C/C_0) = kt$) [13] and was plotted in Fig. 2b. The use of CN/AC-0.3 resulted in the fastest reaction rate (0.07164 min^{-1}), which was 70 times that

of g-C_3N_4 (0.00102 min^{-1}) (Table S2 in Supporting information). The experimental results revealed that the introduction of an appropriate quantity of AC can significantly improve the photocatalytic performance of g-C_3N_4.

The source of the enhanced photoreduction performance of CN/AC composites was explored *via* a series of careful characterizations. The photocatalytic activity of the catalysts was mainly affected by three factors: i) the sunlight absorption range, ii) the specific surface area, and iii) the recombination of photogenerated electron-hole pairs. The UV–vis/DRS results showed that the light absorption range of g-C_3N_4 was wider than that of the CN/AC composites (Fig. S2 in Supporting information), which indicated that widening of the solar light absorption range could not explain the enhanced photocatalytic performance of the CN/AC composites. The specific surface area (SSA) is generally considered to be an important factor affecting photocatalytic activity. Generally, the larger the SSA is, the higher the adsorption performance and the photocatalytic performance are. Unexpectedly, the SSA of CN/AC-0.3 (18.72 m^2/g) was lower than that of g-C_3N_4 (20.52 m^2/g) (Fig. S3 in Supporting information), which meant that the SSA was not a key factor in determining the U(VI) reduction performance. This conclusion was consistent with some reports in the literature [26]. From this point of view, the enhanced photocatalytic performance of CN/AC-0.3 may be attributed to the fast migration of charge carriers. To confirm this speculation, a reliable indicator, *i.e.*, the fluorescence intensity of the catalyst, was used to evaluate the recombination degree of photogenerated electron-hole pairs. In Fig. 2c, the spectra for g-C_3N_4 and CN/AC-0.3 exhibited distinct characteristic peaks at 475 nm, where the peak intensity in the CN/AC-0.3 spectrum was significantly weaker than that in the g-C_3N_4 spectrum, proving that the introduction of AC effectively inhibited the rapid recombination of photogenerated electron-hole pairs. The time-resolved photoluminescence results shown in Fig. 2d provided further strong evidence of the recombination degree of photogenerated electron-hole pairs in the samples. The dynamics of the photogenerated carrier were well fitted by using one fast-component parameter (τ_1) and two slow-component parameters (τ_2 and τ_3). As expected, the lifetime corresponding to the three different τ values of CN/AC-0.3 was much longer than that of g-C_3N_4. More significantly, the proportion of the slow-component parameters (τ_2 and τ_3) increased, while the proportion of the fast-component parameter (τ_1) decreased. These results unequivocally showed that the charge separation and transfer efficiency of CN/AC-0.3 was higher than that of g-C_3N_4 and the recombination of electron-hole pairs was suppressed in CN/AC-0.3. Based on the abovementioned characterization results, it can be concluded that the significant improvement of the photocatalytic performance of CN/AC-0.3 was the considerable inhibition of the rapid recombination of photogenerated electron-hole pairs and the prolonged lifetime of photogenerated charge carriers in CN/AC-0.3.

Batch experiments were carried out to evaluate the U(VI) photoreduction ability of CN/AC-0.3 in different environments. The pH is the main factor affecting uranium species and surface electrical properties [27]. Not surprisingly, photoreduction of U(VI) became difficult at pH 4 (Fig. 3a). Uranium mainly existed as UO_2^{2+} under these conditions, and the electrostatic repulsion between UO_2^{2+} and the positively charged catalyst made it difficult for the catalyst to access uranium [18]. In addition, the large quantity of H^+ in the solution competed with U(VI) for the limited number of electrons [28]. This situation improved significantly as the pH value increased, and the highest photoreduction rate of uranium was obtained at pH 6. However, the reduction performance slightly decreased upon further increasing the pH. This result was obtained because uranium existed as $UO_2(CO_3)_2^{2-}$ and $UO_2(CO_3)_3^{4-}$ under these conditions, resulting in electrostatic repulsion between uranium and the negatively charged catalyst. Overall, the effective

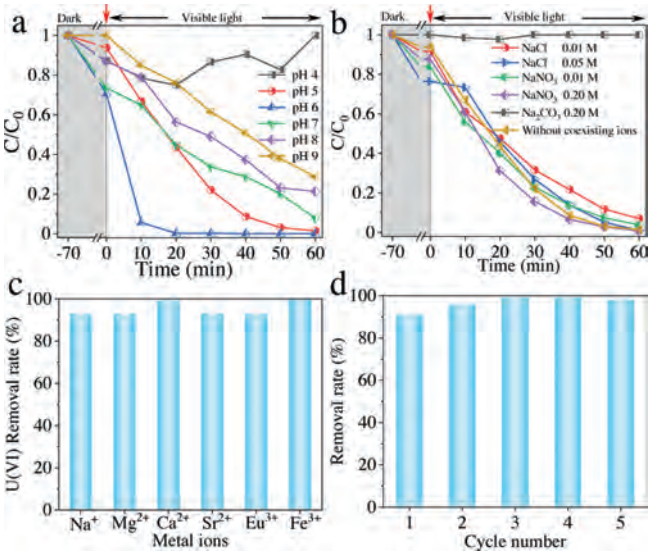

Fig. 3. The photocatalytic performance of CN/AC-0.3. Effect of various pH (a), various anions (b), and cations (c) on photoreduction of U(VI); (d) Cyclic stability of CN/AC-0.3 for photocatalytic removal of U(VI).

photoreduction of U(VI) over a wide pH range made CN/AC-0.3 a potential candidate for uranium removal from radioactive wastewater or alkaline seawater.

For practical application, the influencing factors of competing ions on U(VI) removal must be considered. However, this core issue has not been analyzed in depth. Anions interfere with uranium removal by forming complexes with U(VI). Fig. 3b showed that in the presence of CO_3^{2-}, the photoreduction efficiency of U(VI) was almost negligible because the anion was strongly coordinated with U(VI). The underlying reason for this behavior was that the standard redox potential of uranyl carbonate (−0.69 V) was more negative than that of aqueous uranyl (UO_2^{2+}/U^{4+} (0.267 V), UO_2^{2+}/UO_2 (0.411 V)), which made U(VI) reduction thermodynamically infeasible. Similar experimental results have been previously reported [11]. By contrast, Cl^- promoted the adsorption and photoreduction of U(VI). This result was obtained because the following reaction occurred in the solution: $Cl^- + h^+ \rightarrow Cl^{\bullet}$; that is, Cl^- consumed some of the holes and reduced the recombination rate of the photogenerated charge carriers, thus allowing more electrons to participate in the reduction of U(VI). Furthermore, the addition of a low concentration of NO_3^- (0.01 mol/L) did not affect the photoreduction effect of U(VI). A considerable increase in the NO_3^- concentration to 0.2 mol/L accelerated the U(VI) removal rate. This result may have been obtained because the presence of NO_3^- in the photocatalytic system alleviated the electrostatic repulsion between the U(VI) and the sample. There are many fission products, such as Cs^+ and Sr^{2+}, in radioactive wastewater, and seawater is abundant in Ca^{2+}, Na^+ and K^+. These cations typically compete with uranium, thereby affecting U(VI) removal, and this inhibitory effect becomes more noticeable with increasing ion valence and concentration [29,30]. However, U(VI) removal using CN/AC-0.3 was little affected by various cation interferences, which proved the excellent photoreduction performance of CN/AC-0.3 (Fig. 3c).

Reusability decisively affects the economy and practicality of U(VI) removal. The removal rate of U(VI) by CN/AC-0.3 remained above 90% after 5 cycles of photocatalysis experiments (Fig. 3d). In conclusion, CN/AC-0.3 can adapt to a complex pH environment, had excellent anti-interference to various anions and cations, and more importantly, was economically feasible and practical (being reusable) and can thus be considered a prospective candidate for

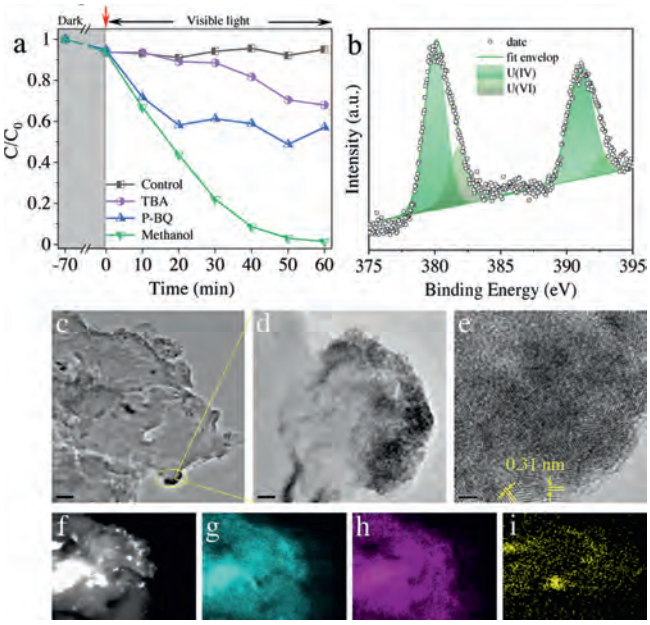

Fig. 4. Exploration of the mechanism of uranium reduction. (a) Effects of various scavengers on photoreduction of U(VI) by CN/AC-0.3, (b) U 4f XPS spectra of used CN/AC-0.3, (c, d) TEM images of the CN/AC-0.3 after photoreduction, and (e) corresponding HRTEM image, (f-i) elemental mapping images of CN/AC-0.3 after photoreduction.

uranium removal recovery from radioactive wastewater and natural seawater.

The mechanism of U(VI) reduction was elucidated by performing quenching experiments (Fig. 4a). TBA, P-BQ, and methanol were selected as trapping agents for $^{\bullet}OH$, $^{\bullet}O_2^-$ and holes (h^+). The introduction of TBA and P-BQ deteriorated the reduction of U(VI). By contrast, U(VI) was rapidly reduced in the presence of methanol. These results showed that the photoreduction of U(VI) was predominantly electron-dependent. The species and sites involved in uranium immobilization were identified by XPS and TEM analyses. Fig. S4 (Supporting information) showed the XPS spectra of fresh and used CN/AC-0.3; the used CN/AC-0.3 spectrum contained a clear U 4f signal, which indicated that uranium was deposited on the catalyst surface. To clarify the valence state of deposited uranium, high-resolution spectra of U 4f were analyzed (Fig. 4b); visual inspection of the spectra showed that U(VI) and U(IV) coexist, and the relative ratios of U(IV) and U(VI) were calculated to be 73% and 27%, respectively. The residual U(VI) may have been produced by reoxidation. Figs. 4c and d showed black particles deposited on the edge of the CN/AC-0.3 composite, and the corresponding HRTEM image showed a distinct lattice fringe with an interplanar spacing of 0.31 nm in line with the (111) plane of UO_2 [31]. The elemental mapping result presented in Figs. 4f-i showed that uranium was evenly distributed at the edge of CN/AC-0.3. Therefore, a reasonable conclusion was that most of the U(VI) was effectively reduced to U(IV) and fixed at the edge of CN/AC-0.3, proving that the method of photocatalytic reduction of U(VI) was effective and feasible.

In summary, a novel low-cost, high-performance carbon-based composite material consisting of carbon nitride/activated carbon (CN/AC) was developed for U(VI) reduction under visible light. The introduction of AC formed a conjugated π-bond structure with g-C_3N_4, expanded the layer spacing of g-C_3N_4, and inhibited the accumulation of g-C_3N_4 layers. CN/AC composites exhibited excellent photocatalytic activity, and the photoreduction rate toward U(VI) was 70 times that of bulk g-C_3N_4, which was attributed to suppression of the recombination of photogenerated electron-hole pairs and prolonged carrier lifetimes. Furthermore, remarkable U(VI) removal capacity was maintained in the presence of competitive anions/cations. The results of cyclic experiments verified the excellent reusability of CN/AC composites. Reduced uranium deposited on the edge of the CN/AC composites was observed by electron microscopy. This low-cost, simple-to-synthesize, and high-performing carbon-based composite material provide a novel and efficient means of treating radioactive wastewater.

Declaration of competing interest

The authors declare that they have no known competing financial interests or personal relationships that could have appeared to influence the work reported in this paper.

Acknowledgments

The financial supports from National Natural Science Foundation of China (No. 22176077), Natural Science Foundation of Gansu Province, China (Nos. 20JR10RA615, 21ZD8JA006), fundamental research funds for the central universities (No. lzujbky-2021-sp29) are acknowledged.

Supplementary materials

Supplementary material associated with this article can be found, in the online version, at doi:10.1016/j.cclet.2022.03.043.

References

[1] H. Zhang, W. Liu, A. Li, et al., Angew. Chem. Int. Ed. 58 (2019) 16110–16114.
[2] C. Wang, A.S. Helal, Z. Wang, et al., Adv. Mater. 33 (2021) e2102633.
[3] H. Wang, H. Guo, N. Zhang, et al., Environ. Sci. Technol. 53 (2019) 6454–6461.
[4] S. Zhang, J. Wang, Y. Zhang, et al., Environ. Pollut. 291 (2021) 118076.
[5] M. Zhao, Z. Cui, D. Pan, et al., ACS Appl. Mater. Interfaces 13 (2021) 17931–17939.
[6] S. Yu, H. Pang, S. Huang, et al., Sci. Total. Environ. 800 (2021) 149662.
[7] H. Li, F. Zhai, D. Gui, et al., Appl. Catal. B: Environ. 254 (2019) 47–54.
[8] C. Liu, P. Hsu, J. Xie, et al., Nat. Energy 2 (2017) 17007.
[9] Y.K. Kim, S. Lee, J. Ryu, et al., Appl. Catal. B: Environ. 163 (2015) 584–590.
[10] S. Lee, U. Kang, G. Piao, et al., Appl. Catal. B: Environ. 207 (2017) 35–41.
[11] Y. Zhang, M. Zhu, S. Zhang, et al., Appl. Catal. B: Environ. 279 (2020) 119390.
[12] T. Chen, B. Liu, M. Li, et al., Chem. Eng. J. 406 (2021) 126791.
[13] P. Li, J. Wang, Y. Wang, et al., Chem. Eng. J. 425 (2021) 131552.
[14] K. Yu, P. Jiang, H. Yuan, et al., Appl. Catal. B: Environ. 288 (2021) 119978.
[15] D. Huang, X. Sun, Y. Liu, et al., Chin. Chem. Lett. 32 (2021) 2787–2791.
[16] X. Zhang, T. Wu, C. Yu, et al., Adv. Mater. 33 (2021) 2104695.
[17] P. Li, Y. Wang, J. Wang, et al., Chem. Eng. J. 414 (2021) 128810.
[18] S. Li, X. Yang, Z. Cui, et al., Appl. Catal. B: Environ. 298 (2021) 120625.
[19] J. Lei, H. Liu, C. Yuan, et al., Chem. Eng. J. 416 (2021) 129164.
[20] T. Chen, J. Zhang, H. Ge, et al., J. Hazard. Mater. 384 (2020) 121383.
[21] Q. Meng, X. Yang, L. Wu, et al., J. Hazard. Mater. 422 (2022) 126912.
[22] Z. Wang, L. Zhang, K. Zhang, et al., Chemosphere 287 (2022) 132313.
[23] S. Lu, F. Liu, P. Qiu, et al., Chem. Eng. J. 379 (2020) 122382.
[24] X. Bai, L. Wang, Y. Wang, et al., Appl. Catal. B: Environ. 152-153 (2014) 262–270.
[25] S. An, G. Zhang, K. Li, et al., Adv. Mater. 33 (2021) 2104361.
[26] D. He, H. Yang, D. Jin, et al., Appl. Catal. B: Environ. 285 (2021) 119864.
[27] P. Li, J. Wang, Y. Wang, et al., J. Photochem. Photobiol. C 41 (2019) 100320.
[28] P. Li, J. Wang, Y. Wang, et al., Chem. Eng. J. 365 (2019) 231–241.
[29] J. Lei, H. Liu, F. Wen, et al., Chem. Eng. J. 426 (2021) 130756.
[30] H. Wan, Y. Li, M. Wang, et al., Chem. Eng. J. 430 (2022) 133139.
[31] J. Wang, Y. Wang, W. Wang, et al., Chem. Eng. J. 383 (2020) 123193.